Long-range atomic order in irradiated $Cu_{80}Mn_{20}$

EUROPHYSICS LETTERS 15 April 2002

Europhys. Lett., **58** (2), pp. 243–249 (2002)

Long-range atomic order in irradiated $Cu_{80}Mn_{20}$

L. D. Cussen[1 2 3], E. MacA. Gray[4], A. P. Murani[1], S. J. Kennedy[3] and B. A. Hunter[3]

[1] *Institut Laue-Langevin - 6 Rue Jules Horowitz, B.P. 156 X Grenoble Cedex 9, France*

[2] *Victoria University of Technology - P.O. Box 14428, MCMC 8001, Australia*

[3] *ANSTO - PMB 1, Menai NSW, 2234, Australia*

[4] *School of Science, Griffith University - Brisbane 4111, Australia*

(received 12 July 2001; accepted in final form 25 January 2002)

PACS. 61.50.Ks – Crystallographic aspects of phase transformations; pressure effects.
PACS. 61.72.Ji – Point defects (vacancies, interstitials, color centers, etc.) and defect clusters.
PACS. 61.80.Hg – Neutron radiation effects.

Abstract. – Atomic short-range order is commonly observed in CuMn alloys via a diffuse $(1\,\frac{1}{2}\,0)$ peak in neutron diffraction patterns. There has been speculation for many years on the existence and nature of any corresponding long-range order. A sample of $Cu_{80}Mn_{20}$ has been irradiated in a high fast-neutron flux to produce a large number of crystal defects at around room temperature and thus facilitate the ordering process. Measurements of the diffuse neutron scattering from this sample demonstrate that long-range order has been induced in the sample, as evidenced by at least five Bragg peaks. This order is not seen in a reference sample prepared in identical fashion except for the irradiation. The Cowley short-range order parameters for both samples are calculated and a candidate structure for the long-range order is proposed.

Introduction. – CuMn alloys display a rich variety of magnetic behaviours and have stimulated interest since the 1930s. Most interest has centred on the γ-phase, a disordered face-centred cubic lattice with a one atom basis, which can be retained at room temperature over a very wide concentration range. A large part of the interest in CuMn has been in the atomic short-range order (ASRO) and accompanying magnetic short-range order shown to be present in the system by many neutron scattering experiments, *e.g.* [1–3]. CuMn alloys are ideal candidates for neutron scattering studies of short-range order because Mn and Cu atoms have similar size and Mn and Cu have large neutron scattering lengths of opposite signs. Short-range order is evidenced by strong diffuse peaks around $(h\frac{k}{2}0)$ (odd k) positions in neutron powder diffraction patterns.

An article by one of the present authors [4] reviewed studies of short-range order in the Cu-rich alloys and its effects on their magnetic properties. In that work a model for the mechanism of atomic short-range ordering in terms of vacancy migration was proposed. Because the energy change during ordering is small, substantial order can be attained only at relatively low temperatures, where the necessary vacancies cluster and annihilate before long-range order can be established. This view is supported by electrical resistivity studies, *e.g.* [5].

Among the studies reported in ref. [4] is one involving irradiation of a $Cu_{83.6}Mn_{16.4}$ sample in a fast-neutron flux. This irradiation was found to drive the atomic short-range ordering at low temperature by increasing the vacancy concentration. It was speculated that a suitable

irradiation could induce long-range order. This is not the only example of neutron irradiation being used to speed up slow atomic ordering processes. For example, fast-neutron irradiation has been used to emulate the effect of the extremely slow cooling of FeNi alloys in meteorites which leads to the formation of tetrataenite [6].

We were led to study the $Cu_{80}Mn_{20}$ composition for two reasons. Firstly, the effectiveness of aging in increasing the low-temperature magnetisation (which correlates with ASRO development [4]) was found to be maximum at this composition [7]. Secondly, Cu_4Mn is one of the superlattices generated by a concentration wave in the (420) series, based on the stacking of (210)-type planes, exhibiting ($\frac{4}{5}\frac{2}{5}0$)-type Bragg peaks. The others are Cu_3Mn ((1 0 0)-type peaks), Cu_2Mn (($\frac{2}{3}\frac{2}{3}0$)-type peaks) and CuMn ((1 $\frac{1}{2}$ 0)-type peaks) [8]. While order based on a [1 $\frac{1}{2}$ 0] lattice wave can directly generate only the CuMn composition, the amplification rate for all lattice waves in the (420) series peaks in $\langle 1\,\frac{1}{2}\,0\rangle$ reciprocal space directions and for this reason a (1 $\frac{1}{2}$ 0) diffuse peak is still expected as a precursor to ordering of FCC A_mB ($m = 2, 3, 4$) by nucleation and growth [8]. Exactly this phenomenon is evident in the FCC Pd-H system [9], where a (1 $\frac{1}{2}$ 0) diffuse peak presages the development of the tetragonal Ni_4Mo superlattice.

Various studies using neutron diffraction have led to claims for underlying structures based on Cu_mMn with $m = 1, 3, 4$. These are reviewed in ref. [10]. The proposal that CuMn microdomains generate the observed ASRO [3, 11] is interesting, as a study of $Cu_{83}Mn_{17}$ by small-angle neutron scattering [12] showed that clusters or microdomains of low dimensionality and radius of gyration about 25 Å exist. Their composition was estimated to be $Cu_{74}Mn_{26}$.

There are several claims in the literature that *ordered* Cu_3Mn or Cu_5Mn has been observed, *e.g.* [13, 14], but these have not been backed up by neutron scattering evidence. Furthermore, as pointed out in ref. [11], the Cu_3Mn structure produces a (100) superlattice peak, which is certainly not apparent in any published data. Khachaturyan [15] showed that any simple superlattice of Cu_5Mn on a FCC lattice would be unstable against the formation of anti-phase boundaries.

Against this background of conflicting claims, our study was devised to determine if the short-range order in $Cu_{80}Mn_{20}$ could be sufficiently enhanced by neutron irradiation near room temperature to induce long-range order and to compare the observed order (if any) with the various models available.

Sample preparation. – The samples were prepared from 99.999% pure copper and 99.98% pure electrolytic manganese. The metals were washed in dilute HNO_3 to remove surface oxide, washed in pure water and dried. Suitable ratios of the metals were weighed and melted in an argon arc furnace. The resulting ingot was cut in the arc furnace, the pieces rearranged and the ingot remelted. This process was repeated five times. The ingot was then sandblasted to remove surface oxide, washed in ethanol under ultrasound and severely cold worked. The ingot was sealed in a silica tube under 150 mbar of argon and homogenised at 900 °C for one week, before being quenched in water. The ingot was again sandblasted and cleaned in ethanol under ultrasound.

A cylinder was turned from the ingot and cut into discs of about 1.5 mm thickness. Six of these discs were clamped in an Al puck which was mounted at the lower end of a "hollow fuel element" irradiation rig and irradiated in the Australian research reactor, HIFAR, for one week. The fast-neutron flux at the sample position was 3.6×10^{12} n/cm^2/s. Because the irradiation rig was positioned in the circulating D_2O, whose temperature is 65 °C, the sample temperature was held close to this figure, which was considerably lower than the estimated temperature of 100 °C used in the previous irradiation experiment [4]. This was expected to be advantageous because it was demonstrated [4] that a greater degree of order could be achieved

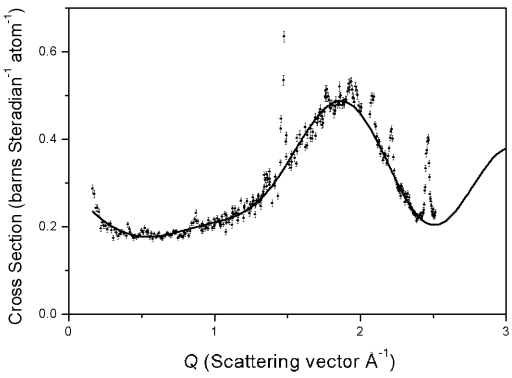

Fig. 1

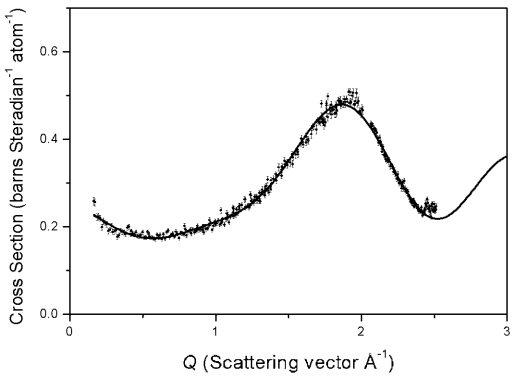

Fig. 2

Fig. 1 – Diffuse coherent plus isotope incoherent scattering from irradiated $Cu_{80}Mn_{20}$ with a fit to the Cowley short-range order parameters as described in the text.

Fig. 2 – Diffuse coherent plus isotope incoherent scattering from the reference non-irradiated $Cu_{80}Mn_{20}$ with a fit to the Cowley short-range order parameters as described in the text.

during aging at a lower temperature and that ordering in the absence of radiation was curtailed by annihilation of the necessary vacancies well before equilibrium was attained. The samples were chosen to be small (2.9 g total mass) to avoid excessive heating during irradiation.

After the irradiation process the samples were found to have a thin black powdery coating, probably CuO. This was not removed due to concerns about the radioactivity of the samples. The samples were left at room temperature for six months for their induced radioactivity to subside. Interestingly, the active isotopes in the sample include a small amount of ^{60}Co, apparently formed by the absorption of a fast neutron by ^{63}Cu followed by an alpha decay. The other long-lived radio-isotopes present (^{54}Mn, ^{65}Zn and ^{110}Ag) are all expected from normal trace impurities in Mn and Cu.

Six other discs of the alloy, chosen to be neighbouring those irradiated but not irradiated themselves, were used to provide the best possible reference sample for comparison.

Measurements. – Measurements were conducted using the D7 polarised neutron diffuse scattering diffractometer at the Institut Laue-Langevin. Using polarised neutrons allows the unambiguous separation of atomic short-range or long-range order from any magnetic order present. The instrument was operated in the "XYZ" polarisation analysis mode [16]. A calibration of the beam polarisation using a quartz sample showed that the instrument had flipping ratios in excess of 35 in all of the 32 detectors used. A vanadium sample was used to normalise detector efficiencies and to provide a reference point for the absolute value of the cross-section. Background scattering was subtracted using a combination of scans taken with an empty sample can and a cadmium sample of the same size and shape as the sample. The calibration was slightly complicated by our using a beam of area $14 \times 17\,\mathrm{mm}^2$ while our sample was a cylinder of average diameter 7 mm and height 10 mm. Thus the relative precision of each point is accurately represented by the error bars but the absolute value of the cross-section is less well characterised and should be assumed to be correct to within 5%. The wavelength used was 4.8 Å. The detectors were stepped 0.5 degrees between points. The measurement was rendered somewhat difficult by the small total sample size and thus a total counting time of over three days on each sample was needed to accumulate adequate counting statistics.

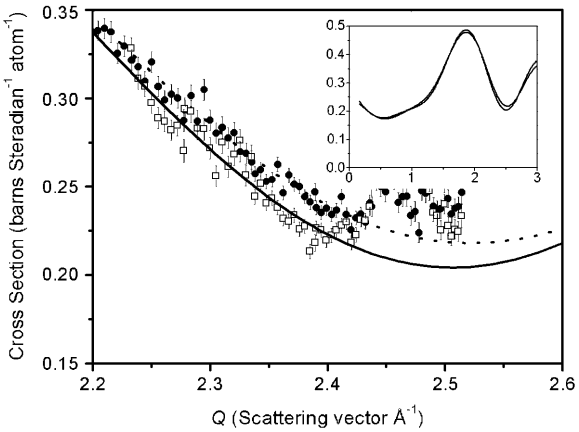

Fig. 3 – Irradiated (open squares) and reference (filled circles) sample data on an expanded scale showing the experimentally significant difference in the short-range order. The inset superimposes the two fits.

Figures 1 and 2 show the diffuse scattering from the irradiated and non-irradiated samples, respectively, at 1.5 K. The points plotted are the sum of the coherent and isotope incoherent cross-sections extracted from the raw data. The lines plotted represent fits to the data which are described below. Both data sets show a clear $(1\,\frac{1}{2}\,0)$ diffuse peak of approximately the same magnitude except that the diffuse hump is somewhat sharper for the irradiated sample than for the reference quenched sample. This is clearly visible in fig. 3 where the fits and an expanded view of both data sets are shown.

An even more remarkable change in the irradiated sample is the existence of several sharp peaks characteristic of a superlattice, hence, the existence of long-range order. These sharp peaks are best viewed as the difference between the data collected and the fit to the short-range order as shown in fig. 4. Five of the peaks evident in fig. 4 were considered reliable and are indicated there. These are the peaks at scattering vectors $Q = 0.87, 1.47, 2.09, 2.21$ and $2.46\,\text{Å}^{-1}$

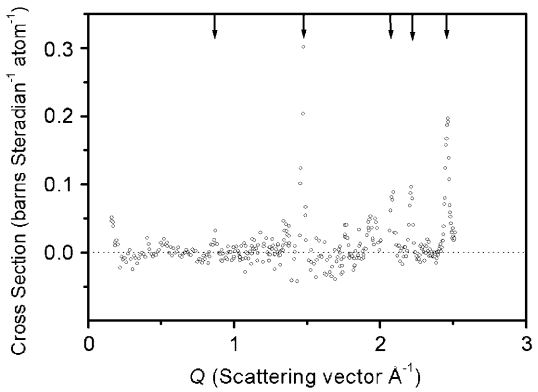

Fig. 4 – The difference between the diffuse scattering from irradiated $Cu_{80}Mn_{20}$ and the short-range order fit showing the Bragg peaks observed. Those marked were assessed as reliable and used to determine a tentative structure.

TABLE I – *Short-range order fitting parameters for the reference and irradiated samples.*

	β_1	α_1	α_2	α_3	α_4	α_5	α_6
Shell	(1/2 1/2 0)	(1/2 1/2 0)	(100)	(1 1/2 1/2)	(110)	(1 1/2 1/2 0)	(111)
Reference	0.002 (4)	−0.097 (5)	−0.01 (1)	0.085 (5)	0.063 (8)	−0.139 (5)	0.25 (2)
Irradiated	0.005 (5)	−0.091 (5)	−0.01 (1)	0.094 (6)	0.083 (9)	−0.167 (5)	0.29 (2)

which index to $(00\frac{1}{2}), (\frac{1}{2}\frac{1}{2}\frac{1}{2}), (\frac{1}{2}\frac{1}{2}1), (\frac{1}{4}\frac{1}{4}\frac{5}{4})/(\frac{3}{4}\frac{3}{4}\frac{3}{4})$ and $(\frac{1}{4}11)/(\frac{1}{2}\frac{1}{2}\frac{5}{4})$ in the conventional cell. There are weaker indications that peaks may be present at $(0\frac{1}{4}\frac{3}{4}), (\frac{1}{4}10), (0\frac{1}{2}1), (\frac{1}{4}\frac{1}{2}1), (\frac{1}{2}\frac{3}{4}1)$ and $(\frac{1}{4}\frac{1}{2}\frac{5}{4})$.

Analysis. – In order to quantify the change in the ASRO peak, the Cowley short-range order parameters have been determined. These are defined by

$$\alpha_i = 1 - \frac{p_i}{c}, \tag{1}$$

for the i-th shell of nearest neighbours where p_i is the probability of finding unlike atoms as i-th nearest neighbours and c is the atomic concentration of the species referred to by p_i. Assuming a Mn atom at the origin, perfect ordering in any shell gives $\alpha_i = 1$ if the shell is completely filled with Mn atoms and -0.25 if the shell is completely filled with Cu atoms.

The Cowley parameters have been extracted by fitting the data to a model derived from the expression for a single crystal [2]:

$$\frac{\mathrm{d}\sigma}{\mathrm{d}\Omega} = A\left[\frac{\sigma_{\mathrm{II}}}{4\pi} + c(1-c)(b_{\mathrm{Mn}} - b_{\mathrm{Cu}})^2\left\{\beta_1 N_1 \frac{\cos(QR_1) - \sin(QR_1)}{QR_1} + \sum_{i=1}^{6} \alpha_i N_i \frac{\sin(QR_1)}{QR_1}\right\}\right]. \tag{2}$$

Here A is an amplitude to compensate for the relatively poor determination of the absolute calibration. In eq. (2), σ_{II} is the isotope incoherent cross-section of the alloy for neutrons and b_{Mn} and b_{Cu} are the coherent scattering lengths. Q is the magnitude of the scattering vector, N_i and R_i are the coordination number and inter-atomic separations for the i-th shell of nearest neighbours and β_1 is the size effect parameter for the first shell. The conventional cubic cell was taken to have a lattice parameter $a_0 = 3.67\,\text{Å}$ as measured at the measurement temperature. The fitting parameters are listed in table I where the numbers in brackets represent the error in the last significant digit. The value of χ^2 was 2.6 for the reference sample and 4.7 for the irradiated sample. The error in each parameter was determined to be the amount by which the parameter had to change to increase χ^2 by 1. The parameter α_0, which must be equal to 1, was allowed to vary in the fit to estimate its error. This provides a test of the modelling. The one sigma confidence limit was found to be 0.02 for both sets of data and this small value is strongly supportive of the fitting procedure used.

In the case of the irradiated sample, points from the five Bragg peaks considered reliable were eliminated from the fit by subtracting simple Gaussian profile fits to the peaks from the data before fitting for short-range order. A maximum of six nearest neighbour parameters could be extracted because of the limited scattering vector range of the data collected. The modelling suggested that a larger number of nearest neighbours is needed to model the data. This is shown by the increasing values of α_i with increasing i.

The Cowley parameters demonstrate the well-known anti-clustering behaviour for nearest neighbours. The differences between the fitting parameters for the reference and irradiated samples are significant —greater than the errors— for α_3, α_5 and α_6. The fact that these changes are most pronounced for the larger radius shells is consistent with developing order

in a superlattice with a large cell. The relatively small size of the changes reflects the small change in the short-range order peak shape.

The possibility that the Bragg peaks arise from oxide contamination —including the black powdery coating on the surface— must be eliminated. Cu and Mn form many oxides including mixed spinel and perovskite compounds. The most common and likely oxide contaminants (CuO, Cu_2O, MnO, MnO_2, Mn_2O_3 and Mn_3O_4) have cells which could not give rise to the Bragg peaks observed. The strongest evidence that the peaks are associated with the sample itself and not some contamination is the near perfect indexing of the peaks to a superlattice of the conventional cell and the observed change in the short-range order. The good comparison of the data with that from the best possible reference sample also strongly supports the contention that the peaks are not an artefact. The observed Bragg peaks cannot be due to λ/n beam contamination which would be present in both the reference and irradiated sample scans.

Modelling the long-range order is clearly a challenging task with a small number of relatively poorly defined Bragg peaks available. The observed peaks are consistent with a tetragonal symmetry in a primitive $4 \times 4 \times 4$ supercell. The highest symmetry space group consistent with the data and the symmetry arguments of ref. [7] is $P\bar{4}n2$ (No. 118). Note that the number of atoms in this cell, 256, is not a multiple of 5 and thus represents a different stoichiometry from Cu_4Mn. The peaks are not consistent with a Ni_4Mo structure and do not correspond to the sharp magnetic peaks reported in ref. [10].

Tetrataenite shows a 0.36% tetragonal distortion from the cubic lattice [6]. Such a tetragonal distortion may accompany the development of long-range order in CuMn, but the present data show no indication of this within the (admittedly coarse) instrument resolution.

Discussion. – The sharpening of the $(1\ \frac{1}{2}\ 0)$ peak following irradiation is consistent with the amplification of this lattice wave when the lattice is perturbed and should be expected prior to the diffuse intensity being diverted into nearby superlattice peaks consistent with the lattice stoichiometry and detailed variation of the atomic interactions. It must be noted, however, that the picture of ASRO provided by fitting the $(1\ \frac{1}{2}\ 0)$ peak with Cowley parameters is incomplete because it mostly excludes the longer-ranged correlations revealed by strong small-angle nuclear scattering [12], the tail of which is just visible in our data. This is hinted at by the increase in the magnitude of the a_i as i increases. This may also explain why our parameters differ considerably from those obtained by analysing data from high-angle volumes of reciprocal space to minimise the magnetic contribution [2, 17].

The small size of the superlattice peaks and the large short-range order peak remaining in the irradiated sample suggest that only a small fraction of the sample is long-range ordered. Given that the induced long-range order appears to be commensurate with the FCC lattice ($4 \times 4 \times 4$ FCC supercell), it seems likely that either the Mn concentration in the ordered regions is much higher than the alloy average, thus limiting the volume of ordered lattice unless gross depletion of Mn in the matrix occurs, or the equilibrium degree of ordering is small at the irradiation temperature of 65 °C. We cannot presently choose between these propositions, although the first is consistent with the small-angle neutron scattering data on $Cu_{83}Mn_{17}$ [12] which reveal the existence of a small volume fraction of clusters or microdomains with Mn concentration higher than average.

In single crystal samples of several alloy systems, for example Ag<u></u>Mn, there are clear indications in the atomic short-range order of satellite structures around the $(1\ \ \frac{1}{2} \pm \delta\ \ 0)$ positions [18, 19]. The effect lessens as the Mn concentration increases. In the case of Cu<u></u>Mn alloys, however, no such distinct satellite peaks have been observed. A slight elongation of the $(1\ \frac{1}{2}\ 0)$ peak along the [1 0 0] direction has been observed for a $Cu_{83}Mn_{17}$ crystal [20] as well

as in a $Cu_{95}Mn_5$ single crystal [21], but the peak shape is almost spherical for the $Cu_{75}Mn_{25}$ alloy [3]. This superstructure is thought to arise in the flattened portions of the Fermi surface in $\langle 1\ 1\ 0\rangle$ k-space directions near the Brillouin zone boundary, causing minima in the Fourier-transformed pair interaction energy to shift slightly from the special points ($\langle 1\ \frac{1}{2}\ 0\rangle$ in this case) dictated by lattice symmetry [8]. Thus it appears that the difference between AgMn and CuMn and the increasing symmetry of the diffuse peak at higher Mn concentrations are Fermi surface effects.

The present work thus raises many interesting questions. The most pressing of these is to confirm the proposed superlattice structure. The magnetic properties of the ordered structure are also clearly of great interest and work on this aspect of the irradiated sample is continuing.

Conclusion. – Measurements of the diffuse scattering from a $Cu_{80}Mn_{20}$ sample subjected to intense fast-neutron irradiation show a change in the atomic short-range order accompanied by the development of atomic long-range order in a superlattice of $4\times4\times4$ conventional cubic unit cells.

* * *

We thank Mr. D. Hurwood and Mr. R. Law of ANSTO for their essential help in arranging the sample irradiation. Dr. R. Stewart of ILL provided enthusiastic and helpful support in the use of D7. LDC thanks Dr. A. R. Wildes for assistance.

REFERENCES

[1] Meneghetti D. and Sidhu S. S., *Phys. Rev.*, **105** (1957) 130.
[2] Wells P. and Smith J. H., *J. Phys. F*, **1** (1971) 763.
[3] Cable J. W., Werner S. A., Felcher G. P. and Wakabayashi N., *Phys. Rev. B*, **29** (1984) 1268.
[4] Gray E. and Mac A., *J. Phys. Condens. Matter*, **8** (1996) 751.
[5] Kahl S., Neuhaus R., Pinkvos H. and Schwink C., *Phys. Status Solidi A*, **120** (1990) 221.
[6] Albertsen I. F., *Phys. Scr.*, **23** (1981) 301.
[7] Gibbs P., Harders T. M. and Smith J. H., *J. Phys. F*, **15** (1985) 213.
[8] de Fontaine D., *Acta Metall.*, **23** (1975) 553.
[9] Wu E., Kennedy S. J., Gray E. MacA. and Kisi E. H., *J. Phys. Condens. Matter*, **8** (1996) 2807.
[10] Tsunoda Y. and Cable J. W., *Phys. Rev. B*, **46** (1992) 930.
[11] Bouchiat H., Dartyge E., Monod P. and Lambert M., *Phys. Rev. B*, **23** (1981) 1375.
[12] Gray E. and Mac A., Hicks T. J. and Smith J. H., *J. Phys. F*, **12** (1982) L189.
[13] Warlimont H., Bernecker K. and Lück R., *Z. Metall.*, **62** (1971) 816.
[14] Gödecke T., *Z. Metall.*, **81** (1990) 826.
[15] Khachaturyan A. G., *Phys. Status Solidi B*, **60** (1973) 9.
[16] Schärpf O. and Capellmann H., *Phys. Status Solidi A*, **135** (1993) 359.
[17] Hirabayashi M., Koiwa M., Yamaguchi S. and Kamata K., *J. Phys. Soc. Jpn.*, **45** (1978) 1591.
[18] Bouchiat H. and Dartyge E., *J. Phys. (Paris)*, **43** (1982) 1699.
[19] Koga K., Ohshima K. and Niimura N., *Phys. Rev. B*, **47** (1993) 5783.
[20] Roelofs H., Schoenfeld B., Kostorz G., Buhrer W., Robertson J. L., Zschack P. and Ice G. E., *Scr. Mater.*, **34** (1996) 1393.
[21] Murani A. P., Scharpf O., Andersen K. H., Richard D. and Raphel R., *Physica B*, **267-268** (1999) 131.